

# Pre-melting of crossing vortex lattices

S. BUTSCH<sup>1</sup>, E. ZELDOV<sup>2</sup> and T. NATTERMANN<sup>3</sup>

<sup>1</sup> *Miamed GmbH - Köln, Germany*

<sup>2</sup> *Weizmann Institute of Science - Rehovot 76100, Israel*

<sup>3</sup> *Institut für Theoretische Physik, Universität zu Köln - Köln, Germany*

received 21 June 2013; accepted in final form 6 August 2013

published online 16 September 2013

PACS 74.25.Uv – Vortex phases (includes vortex lattices, vortex liquids, and vortex glasses)

PACS 74.25.Op – Mixed states, critical fields, and surface sheaths

PACS 74.25.Dw – Superconductivity phase diagrams

**Abstract** – The pre-melting of high vortex density planes observed recently in layered superconductors in tilted magnetic field (SEGEV Y. *et al.*, *Phys. Rev. Lett.*, **107** (2011) 247001) is explained theoretically. Based on the structural information of the crossing lattices of pancake and Josephson vortices the effective vortex cage potential at different lattice sites is determined numerically. Melting takes place when the thermal energy allows proliferation of vacancy-interstitial pairs. It is found that the increased density of pancake vortex stacks in the planes containing Josephson vortices, rather than their incommensurate structure, is the main cause for pre-melting.

Copyright © EPLA, 2013

**Introduction.** – Melting of solids, an everyday phenomenon from the shrinking ice cube in a drink to the processes in the Earth mantle, is far from being well understood. At the melting transition the shear modulus of the material vanishes [1]. There are several phenomenological criteria predicting when this will happen (see [1–3] for a discussion). Most prominent is the Lindemann criterion [4], stating that melting occurs when the mean square fluctuation of the atoms in a solid is a fraction  $c_L$  (the Lindemann number) of the interatomic distance. On a more conceptual level it is expected that the proliferation of defects or grain boundaries plays an important role in melting. In two dimensions melting was indeed shown to be a two-stage process, driven by unbinding of dislocations and disclinations, respectively [5], while in three dimensions a sudden increase of the vacancy concentration was observed at the transition [2,6–8].

In this letter we address the question of the melting process in a heterogeneous system. Since inhomogeneities and extended defects occur naturally in any practical system, comprehension of the melting transition in such systems is of broad importance. Vortex lattices in superconductors have been extensively utilized as a model system for theoretical and experimental studies of the melting transition [9,10]. The melting line in (isotropic) superconductors is parametrized by the dimensionless ratio  $\epsilon_T = \lambda/\Lambda_T$ . Here  $\lambda$  denotes the London penetration depth and  $\Lambda_T = \phi_0^2/(16\pi^2 k_B T)$  is a thermal length scale,

only related to the temperature  $T$  and the flux quantum  $\phi_0 = hc/(2e)$ . In high- $T_c$  materials with their elevated transition temperatures and large values of  $\lambda$ ,  $\epsilon_T$  can become of order one, replacing a large part of the mean-field phase diagram by the vortex liquid phase [11].

An additional and qualitative new aspect appears in extremely anisotropic systems like  $\text{Bi}_2\text{Sr}_2\text{CaCu}_2\text{O}_{8+\delta}$  (BSCCO), which are composed of alternating normal and superconducting layers. Vortex lines perpendicular to the layers consist of stacks of pancake vortices (PVs), residing in the superconducting layers, whereas the coupling between them is mainly of electromagnetic origin. Vortex lines parallel to the layers take advantage of normal regions and are hence Josephson vortices (JVs) [12,13]. Denoting the layer period by  $s$ , two further dimensionless ratios,  $\lambda_{ab}/s \equiv \epsilon_s$  and  $\lambda_c/\lambda_{ab} \equiv \gamma$ , characterize the system ( $\epsilon_s \gtrsim 130$  and  $\gamma \approx 500$  in BSCCO).  $\lambda_c$  and  $\lambda_{ab}$  denote the out-of-plane and in-plane penetration depth, respectively.

When the magnetic field is tilted away from the  $c$ -axis, chains of higher vortex density were found in Bitter decorations [14–16], scanning Hall probe microscopy [17,18], Lorentz microscopy [19], and magneto-optical imaging [20–22], and described as crossing lattices of pancake and Josephson vortices (see fig. 1(a)) [23–29]. The resulting vortex lattice structure displays a very rich phase diagram that depends critically on the strength and direction of the magnetic field  $\mathbf{H}$  and on the ratio of  $\epsilon_s/\gamma$ .

It was recently found [30] that in a tilted magnetic field the melting transition in BSCCO changes from a homogeneous first-order process into a two-step transition that is apparently driven by an intrinsic heterogeneity of the vortex lattice structure. Melting occurs first in the planes containing the Josephson vortices (henceforth called Josephson planes), creating an intermediate periodic solid-liquid state [30]. The previous theoretical studies of the melting of the crossing lattices [23–28] have investigated the global behavior assuming a *single* melting transition. It is therefore the goal of the present work to give a first theoretical explanation for this effect.

In its full generality this a very difficult task. The frequently used Lindemann criterion cannot be applied in the present case since it requires the knowledge of the spatial dependence of the elastic constants, resulting from the superstructure of the flux line lattice. However, since the Lindemann criterion is dominated by the physics on short length scale it seems to be obvious to apply a *local* theory. Consequently, in this paper we will calculate the effective cage potential, acting on a given PV due to its interaction with all other vortices. In doing this we will replace the instantaneous positions of the surrounding vortices by their equilibrium ones. Melting is concluded to occur at temperatures where the PV under consideration can escape from the cage potential via its lowest saddle point, triggering proliferation of vacancy-interstitial pairs. This happens first for PVs in the Josephson planes. The melting temperature determined in this way is in reasonable agreement with the experimental findings.

**Model.** – We follow here the conclusions of [28] that the discrete layer structure has strongest influence on the cores of tilted and Josephson vortices, but that interaction contributions to the total energy usually can be computed within continuous approximation. PVs and JVs in their equilibrium position can be considered to be threaded on a contour line  $\mathbf{r}_i(t)$ . The vorticity  $\boldsymbol{\omega}$  of the lattice can be written as

$$\boldsymbol{\omega}(\mathbf{r}) = \sum_i \int dt (d\mathbf{r}_i(t)/dt) \delta(\mathbf{r} - \mathbf{r}_i(t)), \quad (1)$$

which is related to the magnetic induction  $\mathbf{B}$  by

$$\mathbf{B} + \nabla \times \sum_{\alpha} \lambda_{\alpha}^2 (\nabla \times \mathbf{B})_{\alpha} \hat{r}_{\alpha} = -\phi_0 \boldsymbol{\omega}(\mathbf{r}). \quad (2)$$

Here  $\lambda_z \equiv \lambda_c$  and  $\lambda_x = \lambda_y \equiv \lambda_{ab}$ . The free energy  $\mathcal{F}$  of vortex systems is a functional of the vorticity field which includes contributions both from the magnetic and the Josephson interaction [28]

$$\mathcal{F}[\boldsymbol{\omega}] = \frac{\phi_0^2}{8\pi} \int \frac{d^3k}{(2\pi)^3} \frac{|\boldsymbol{\omega}_{\mathbf{k}}|^2 + \lambda_{ab}^2 k^2 (\gamma^2 |\omega_{z\mathbf{k}}|^2 + |\boldsymbol{\omega}_{\perp\mathbf{k}}|^2)}{(1 + \lambda_{ab}^2 k^2) [1 + \lambda_{ab}^2 (k_z^2 + \gamma^2 \mathbf{k}_{\perp}^2)]}. \quad (3)$$

$\boldsymbol{\omega}_{\mathbf{k}}$  is the Fourier transform of  $\boldsymbol{\omega}(\mathbf{r})$ . The subscript  $\perp$  denotes the projection of a vector onto the  $xy$ -plane. The

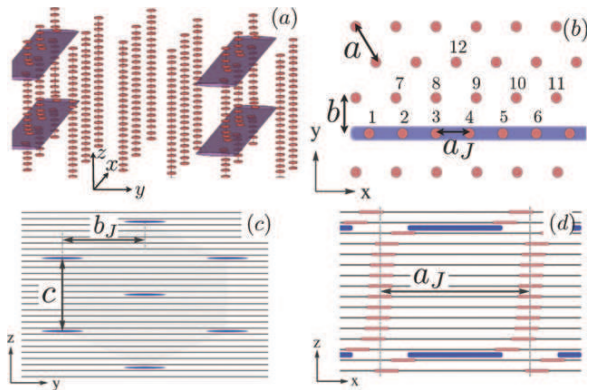


Fig. 1: (Colour on-line) (a) Schematic 3D plot of the crossing PV-JV lattice. The JVs are aligned along the  $x$ -axis and are stacked along  $z$  forming “Josephson planes” along  $xz$ -planes. (b) Top view ( $xy$ -plane) of the PVs (red) and JVs (blue). The vortex numbers are used in figs. 2 and 3. (c) Front view of the JV lattice ( $yz$ -plane). (d) Side view of PVs and JVs in the Josephson plane ( $xz$ -plane).

actual equilibrium flux lattice structure follows from the minimization of

$$\mathcal{F}[\boldsymbol{\omega}] - \int d^3r \mathbf{B} \cdot \mathbf{H} / 4\pi \quad (4)$$

for a given magnetic field  $\mathbf{H}$ .

Once the equilibrium structure is known, the effective potential for a pancake vortex displacement  $\mathbf{u}_{i,n}$  in stack  $i$  and layer  $n$  can be found from the change of the vorticity field  $\Delta\boldsymbol{\omega}(\mathbf{r})$  in (3). Its Fourier transform is  $\Delta\boldsymbol{\omega}_{\mathbf{k}} = \hat{z} s e^{i\mathbf{k}\cdot\mathbf{r}_i} [e^{i\mathbf{k}_{\perp}\cdot\mathbf{u}_{i,n}} - 1]$ . This allows to calculate the free-energy change  $\Delta\mathcal{F}(\mathbf{u}_{i,n})$  which depends in general on  $i$  and  $n$ . The actual vortex structure in the Josephson planes consists of continuous vortex lines formed of stacks of PVs, connected by JVs, as indicated in fig. 1(d) [28,31]. The resulting discontinuity of the JVs in a single plane (and hence also the displacements of the PVs from a straight stack) is of the order  $\lambda_{ab}\epsilon_s / [(2n-1)\gamma]$  [31], which is for our parameter values  $\lesssim 0.06 a_J/n$ .  $n \geq 1$  denotes the number of layers between the JVs [31]. We will therefore ignore in the following this small effect and assume a simple crossing lattice of straight stacks of PVs and straight JVs [32].

**Effective cage potential.** – Displacing a single PV from a straight stack generates an antiparallel pair of JVs in the adjacent non-superconducting layers. Because of their large mutual annihilation, the interaction of this excited JV pair with the static JVs of the crossing lattice will be very small, provided the displaced PV is not too close to the JV. We will ignore this weak interaction in the following as well. With these approximations,  $\hat{\omega}$  of PV and JVs are now perpendicular to each other, and hence Josephson vortices do not contribute to the effective potential of the displaced pancake vortices once the

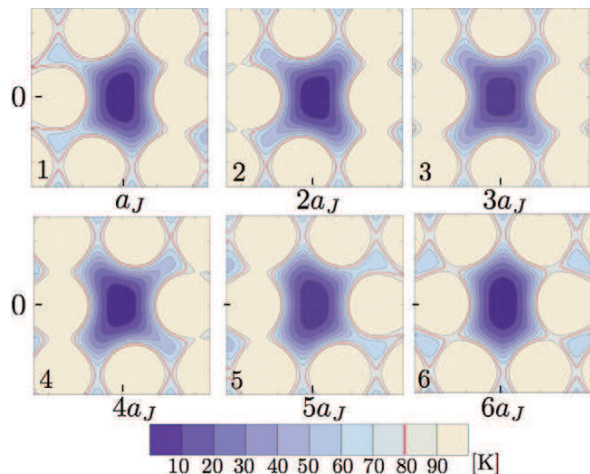


Fig. 2: (Colour on-line) Set of contour plots of the cage potential  $\Delta\mathcal{F}(\mathbf{u}_i)$  for a single displaced PV in a stack of PVs in the Josephson plane for the different stacks numbered as in fig. 1(b). Only the PV with rest position in the center is assumed to be displaced, keeping all other PVs at their equilibrium positions. With the choice of  $a_J/a = 5/6$  this sequence is repeated every 6 stacks.

structure is fixed. Moreover, the effective potential for a single displaced PV does not depend on its position in the stack. This approximation is justified the more the larger the distance between the displaced PV and the JV.

After summation over the PVs in the stacks and suppressing the layer index  $n$ , the effective cage potential  $\Delta\mathcal{F}[\mathbf{u}_i]$  for a single PV, displaced from a straight stack by  $\mathbf{u}_i$ , can be written in the form

$$\Delta\mathcal{F} = \frac{k_B T}{\epsilon_T \epsilon_s} \sum_{j(\neq i)} [K_0(|\mathbf{R}_{ij} - \mathbf{u}_i|/\lambda_{ab}) - K_0(R_{ij}/\lambda_{ab})]. \quad (5)$$

Here  $K_0(x)$  is the modified Bessel function,  $\mathbf{R}_{ij}$  the position vector connecting stacks  $i$  and  $j$ , and  $R_{ij} = |\mathbf{R}_{ij}|$ . In addition there is a small entropic contribution  $-2T \ln(a/\xi)$  to the free energy. The remaining sum has to be performed numerically which requires the knowledge of the flux lattice structure. Both analytical theory [28] and experimental findings [14] are consistent with the following *reference* flux lattice structure:

- Vortices are located in planes parallel to the  $xz$ -plane ( $H_y = 0$ ) (compare fig. 1(a), (b)).
- PV stacks outside the Josephson planes form a equilateral triangular lattice of spacing  $a$  [15,25].
- The PV distance in the Josephson planes is denoted by  $a_J (< a)$  and the distance between Josephson and the adjacent planes by  $b (> \sqrt{3}a/2)$  (fig. 1(b)).  $a_J < a$  is the result of the attractive interaction between PVs and JVs.

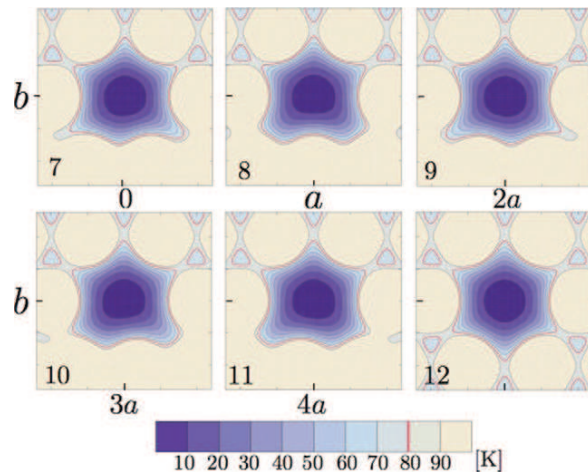


Fig. 3: (Colour on-line) Contour plot of  $\Delta\mathcal{F}$  for PVs in the plane adjacent to the Josephson plane (numbered 7 to 11 in fig. 1(b)) and in the bulk (number 12). Melting occurs at about 10 K higher than for PVs in the Josephson plane in fig. 2.

- The projection of the JVs onto the  $yz$ -plane forms squeezed Abrikosov lattice with the lattice parameter ratio  $b_J/c = \sqrt{3}\gamma/2$  (compare fig. 1(c)).

Although the reference structure is taken here as an additional input we will show below that relaxing these conditions results only in weak deviations from the assumed configuration.

Figure 2 shows the results of the calculation of the free-energy change  $\Delta\mathcal{F}$  due to the displacement of the individual PVs in the Josephson plane labeled 1 to 6 in fig. 1(b). Here we used the lattice parameters found in the Bitter decoration experiment [14] performed in BSSCO at  $\mathbf{H} = (30, 0, 24)$  Oe where  $a = 1$ ,  $a_J = 0.833$ ,  $b = 0.91$ ,  $c = 0.04$ ,  $b_J = 17.32$ ,  $\lambda_{ab}(T) = \lambda(0)\sqrt{1 - T/T_c}$ ,  $\lambda(0) = 0.2$ , all lengths in  $\mu\text{m}$ . The value of  $H_x$  is slightly larger than that used in [30]. Since in the present case  $a_J/a = 5/6$ , the potential shapes recur every six vortices. The contour maps of lines of constant energy are depicted in units of  $k_B T$ . There are two important observations here. First, although the precise shape of the potential is different for the individual vortices, saddle points with very similar value  $T \approx 75$  K appear for all the locations. At this temperature PVs can escape in direction transverse to the Josephson plane, vacancy-interstitial pairs proliferate, and the lattice starts to melt along the Josephson planes. This transverse melting process appears to be uniform for the various PVs along the Josephson plane. The second observation is that in contrast to the transverse direction, the shape of the potential along the Josephson plane is rather position dependent. Vortices that are located at symmetric points that are in registry with the adjacent planes, like vortex 3 and 6, show potential that is quite localized in the  $x$ -direction. On the other hand, the potentials at asymmetric locations, like vortex 1 and 5,

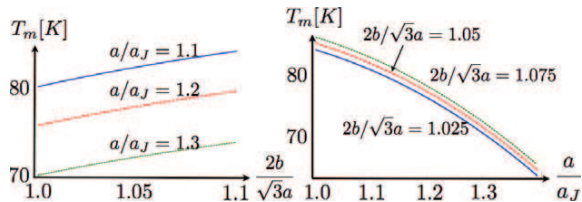


Fig. 4: (Colour on-line) Melting temperature of PVs along the Josephson planes  $T_m$  in a crossing lattices state with regular lattice parameter  $a = 1 \mu\text{m}$  as a function of  $b/a$  (left panel) and of  $a/a_J$  (right panel).

show extended protrusions that indicate enhanced vortex mobility at the less-stable vortex positions along the Josephson planes. This finding can explain the apparent observation of site-dependent enhancement of vortex fluctuations along the Josephson planes in Lorentz microscopy studies [19] that was discussed in terms of the incommensurability of the vortex chains structure.

The corresponding pictures for PVs in the plane adjacent to the Josephson plane are shown in fig. 3 along with PV number 12 in the bulk. Despite the fact that each of the PVs has a different local energy landscape, it is clearly seen that all the PVs can leave their positions only at temperatures of  $T_m \simeq 85 \text{ K}$ , 10 K higher than the PVs in the Josephson planes. The experimental bulk melting temperature is  $T_m \approx 90 \text{ K}$ . A remark is in order: since the vortex cage potential is calculated with all surrounding vortices in their equilibrium positions, proliferation is predominant in the direction perpendicular to the Josephson plane. We expect that in a treatment which allows simultaneous motion of all vortices this prevalence is reduced.

Figure 4 shows a detailed calculation of the melting temperature  $T_m$  of the PVs in the Josephson planes as a function of their intervortex distance  $a_J$  and the separation  $b$  between the Josephson plane and the adjacent PV plane (see fig. 1(b)).  $T_m$  is found to drop rapidly with increasing  $a/a_J$  and with decreasing  $b/a$  giving rise to pre-melting of the Josephson planes that could in principle be as large as 20 K. In reality, however,  $a_J$  and  $b$  are not independent parameters and are both determined by  $H_x$  and  $H_z$ . In particular, increasing  $H_x$  decreases  $a_J$  but increases  $b$ , so that the two dependences moderate each other to a large extent. We therefore expect a much smaller pre-melting as observed experimentally [30].

**Distortions from the reference structure.** – So far we assumed for the vortex lattice structure the reference structure taken from decoration experiments. We will now study possible deviations from this configuration. As an example we consider deviations from the assumed equidistant vortex positions in the Josephson plane by replacing  $a_J$  by  $a_J(n)$ . Here  $n$  numbers the intervals. The  $a_J(n)$  follow from the competition between the PV-JV interaction in the Josephson plane on one side, which favors a lattice spacing smaller than  $a$ , and their interaction with

the PVs outside the Josephson plane on the other side, which favor registry with the lattice constant  $a$ , which we assume to be fixed. Such a system can be described by the Frenkel-Kontorowa model [33],

$$\mathcal{H} = \sum_n [(\theta_{n+1} - \theta_n - \delta)^2 - 2\zeta \cos \theta_n]. \quad (6)$$

The  $\theta_n$  describe the modulation of the PV positions,  $x_n = an + a\theta_n/(2\pi)$ ,  $\zeta = 2\pi^2 k_2/(q^2 k_1)$ , and  $q = a/\lambda_{\text{ab}}$ . The misfit parameter  $\delta < 0$ , depending on  $H_x$ , favors a higher PV density in the Josephson planes. It will be determined below from the average vortex spacing  $\langle a_J(n) \rangle \equiv a_J$ . The coefficient  $k_1$  follows from the vortex interaction as  $k_1 = K_0(q) + q^{-1}K_1(q)$ .  $k_2$  is determined numerically by fitting the actual vortex interaction of a Josephson plane stack with its neighboring stacks in the satellite plane to a cosine model, taking up to the fifth next neighbour into account. The ground state configuration follows from the saddle point condition  $\theta_{n+1} + \theta_{n-1} - 2\theta_n = \zeta \sin \theta_n$ . In the continuum limit,  $\theta_n \rightarrow \theta(n)$ , one arrives at the rigid pendulum equation  $\theta''(n) = \zeta \sin \theta$ . Its solution can be expressed by elliptic functions which depend on the constant of integration  $\eta$ .  $\eta$  follows from the minimization of  $K(\eta^2 - 2) + 4E - \pi\delta\eta/\sqrt{\zeta}$ . Here  $K(\eta)$  and  $E(\eta)$  are the complete elliptic integrals of first and second kind, respectively. For small misfit,  $|\delta| < \delta_c = 4\sqrt{\zeta}/\pi$ ,  $\theta(n)$  locks-in at a multiple of  $2\pi$ , corresponding to  $a_J = a$ . For  $|\delta| \gtrsim |\delta_c|$  the solution for  $\theta(n)$  is staircase-like with horizontal terraces at  $\theta(n) \approx 2\pi p$  ( $p \in \mathbb{N}$ ), which are connected by steps of width  $\sim \zeta^{-1/2}$ . The average PV spacing in the Josephson plane is in general incommensurate with  $a$ . For a given  $a_J$ ,  $\delta$  is determined from the relations  $a_J = a[1 - \sqrt{\zeta}/(2\eta K)]$  and  $\eta = 4\sqrt{\zeta}E/(\pi\delta)$ . With the parameter values given above we get  $\zeta = 0.409$ ,  $|\delta_c| = 0.814$ ,  $\eta = -0.876$  and  $\delta \approx -1.115$ . Thus the system is indeed in the incommensurate phase in which the PV distance is modulated. However this modulation of  $a_J(n)$  is less than 6% of the mean vortex distance and hence can be safely ignored for the investigation of the melting transition. We expect that similar weak deviations from the reference structure appear when other lattice parameters are allowed to deviate from the reference structure.

**Conclusions.** – In summary, using a cage potential model we have calculated the melting temperature of the PVs at different locations in the crossing lattices state parametrized by three different lattice constants  $a$ ,  $a_J$ ,  $b$ . Detailed results were obtained for a reference PV lattice structure relevant to highly anisotropic superconductor BSCCO. We showed that melting of crossing flux line lattices sets in along the planes containing JVs where the local melting temperature can be substantially lower than in the bulk resulting in a periodic solid-liquid structure as observed experimentally [30]. We also have analyzed the effect of a possible incommensurate modulation of the PV lattice constant  $a_J$  along the Josephson plane and found it to be too weak to have a significant effect on the melting

transition. The primary cause of the pre-melting transition is the proliferation of vacancy-interstitial PV pairs at reduced temperatures due to the increased PV density along the Josephson planes.

\* \* \*

We thank A. KOSHELEV for useful discussions. This work was supported by the German-Israeli Research Foundation (I-1030-14.14/2009) and the Deutsche Forschungsgemeinschaft (SFB 608).

#### REFERENCES

- [1] BORN M., *J. Chem. Phys.*, **7** (1939) 591.
- [2] CAHN R. W., *Nature*, **273** (1978) 491.
- [3] MEI Q. S. and LU K., *Prog. Mater. Sci.*, **52** (2007) 1175.
- [4] LINDEMANN F. A., *Phys. Z.*, **11** (1910) 609.
- [5] NELSON D. R. and HALPERIN B. I., *Phys. Rev. B*, **19** (1979) 2457.
- [6] FRENKEL J., *J. Chem. Phys.*, **7** (1939) 538.
- [7] FRENKEL Y. I., *Kinetic Theory of Liquids* (Dover, New York) 1955.
- [8] GORECKI T., *Z. Metallkd.*, **67** (1976) 269.
- [9] BLATTER G., FEIGEL'MAN M. V., GESHKENBEIN V. B., LARKIN A. I. and VINOKUR V. M., *Rev. Mod. Phys.*, **66** (1994) 1125.
- [10] ZELDOV E., MAJER D., KONCZYKOWSKI M., GESHKENBEIN V. B., VINOKUR V. M. and SHTRIKMAN H., *Nature*, **375** (1995) 373.
- [11] SUDBØ A. and BRANDT E. H., *Phys. Rev. B*, **43** (1991) 10482.
- [12] CLEM J. R., *Phys. Rev. B*, **43** (1991) 7837.
- [13] BULAEVSKII L. N., LEDVIJ M. and KOGAN V. G., *Phys. Rev. B*, **46** (1992) 366, 11807.
- [14] BOLLE C. A. *et al.*, *Phys. Rev. Lett.*, **66** (1991) 112.
- [15] GRIGORIEVA I. V., STEEDS J. W., BALAKRISHNAN G. and PAUL D. M., *Phys. Rev. B*, **51** (1995) 3765.
- [16] TOKUNAGA M., TAMEGAI T., FASANO Y. and DE LA CRUZ F., *Phys. Rev. B*, **67** (2003) 134501.
- [17] GRIGORENKO A., BENDING S., TAMEGAI T., OOI S. and HENINI M., *Nature*, **414** (2001) 728.
- [18] GRIGORENKO A. N., BENDING S. J., KOSHELEV A. E., CLEM J. R., TAMEGAI T. and OOI S., *Phys. Rev. Lett.*, **89** (2002) 217003.
- [19] MATSUDA T., KAMIMURA O., KASAI H., HARADA K., YOSHIDA T., AKASHI T., TONOMURA A., NAKAYAMA Y., SHIMOYAMA J., KISHIO K., HANAGURI T. and KITAZAWA K., **294** (2001) 2136.
- [20] VLASKO-VLASOV V. K., KOSHELEV A., WELP U., CRABTREE G. W. and KADOWAKI K., *Phys. Rev. B*, **66** (2002) 014523.
- [21] TOKUNAGA M., KOBAYASHI M., TOKUNAGA Y. and TAMEGAI T., *Phys. Rev. B*, **66** (2002) 060507.
- [22] SEGEV Y., GUTMAN I., GOLDBERG S., MYASOEDOV Y., ZELDOV E., BRANDT E. H., MIKITIK G. P., KATAGIRI T. and SASAGAWA T., *Phys. Rev. B*, **83** (2011) 104520.
- [23] HUSE D. A., *Phys. Rev. B*, **46** (1992) 8621.
- [24] KOSHELEV A. E., *Phys. Rev. B*, **48** (1993) 1180.
- [25] KOSHELEV A. E., *Phys. Rev. Lett.*, **83** (1999) 187.
- [26] DODGSON M. J. W., *Phys. Rev. B*, **66** (2002) 014509.
- [27] KOSHELEV A. E., *Phys. Rev. B*, **68** (2003) 094520.
- [28] KOSHELEV A. E., *Phys. Rev. B*, **71** (2005) 174507.
- [29] BENDING S. J. and DODGSON M. J. W., *J. Phys.: Condens. Matter*, **17** (2005) R955.
- [30] SEGEV Y., MYASOEDOV Y., ZELDOV E., TAMEGAI T., MIKITIK G. P. and BRANDT E. H., *Phys. Rev. Lett.*, **107** (2011) 247001.
- [31] BUZDIN A. and BALADI I., *Phys. Rev. Lett.*, **88** (2002) 147002.
- [32] DODGSON M. J., *Physica C: Supercond.*, **369** (2002) 182.
- [33] FRENKEL J. and KONTOROWA T., *Phys. Z. Sowjet.*, **13** (1938) 1.